

TIME-DEPENDENT BEHAVIOUR OF REINFORCED CUTS IN WEATHERED FLYSCH ROCK MASSES

MIRKO GROŠIĆ and ŽELJKO ARBANAS

about the authors

Mirko Grošić
Geotech Ltd.
Moše Albaharija 10a, 51000 Rijeka, Croatia
E-mail: mirko.grosic@geotech.hr

Željko Arbanas
University of Rijeka,
Faculty of Civil Engineering
Radmile Matejčić 3, 51000 Rijeka, Croatia
E-mail: zeljko.arbanas@gradri.uniri.hr

abstract

Knowledge of stress-strain rock mass behaviour is crucial for many engineering purposes. Rock mass deformations and their influences on construction are observed during construction and even during exploitation phases. These deformations in the exploitation phase are caused by the time-dependent behaviour of the rock mass. A flysch rock mass is categorised as a heterogenic weak rock that has been intensely subjected to weathering processes. Due to weathering processes, the flysch rock mass degrades from fresh rock to residual soil within only a few meters of the geological profile below the surface. Observations of reinforced cuts along the Adriatic motorway near the City of Rijeka, Croatia, were conducted over a time period of seven years of spanning construction and exploitation. Measured displacements reached significant magnitudes during the exploitation period as a consequence of the time-dependent behaviour of the rock mass. The paper presents findings related to flysch rock mass weathering profile and its characteristics based on detailed geotechnical investigations and monitoring results coupled with back analyses. It was found possible to detect the thickness of the flysch rock mass weathering profile by performing detailed geotechnical investigations. Recommendations for the strength, deformation, and creep properties of the weathering profile of a flysch rock mass are given.

keywords

time-dependent behaviour, weathering, weak rock mass, Burger model, back analyses

1 INTRODUCTION

CREEP MECHANICS

According to Hackley and Ferraris [1], rheology is the science of the deformation and flow of matter. The term creep is used to describe the response of a material to the instantaneous application of a constant stress. The term creep refers to intact rock, whereas the term time-dependent behaviour refers to the much larger volume of a rock mass. A rock mass consisting of intact rock and discontinuities is extremely heterogeneous compared with intact rock; therefore, the term time-dependent behaviour consolidates all these factors.

In creep mechanics, there are three different phases—primary, secondary or stationary, and tertiary creep phases—which are presented in Fig. 1. These three phases correspond to decreasing, stationary, and increasing creep strain rates, respectively, and were introduced by Andrade [2]. Immediately after applying a load, an instantaneous elastic strain occurs, followed by the primary creep phase. It is a delayed process and is recoverable after unloading. After this primary phase,

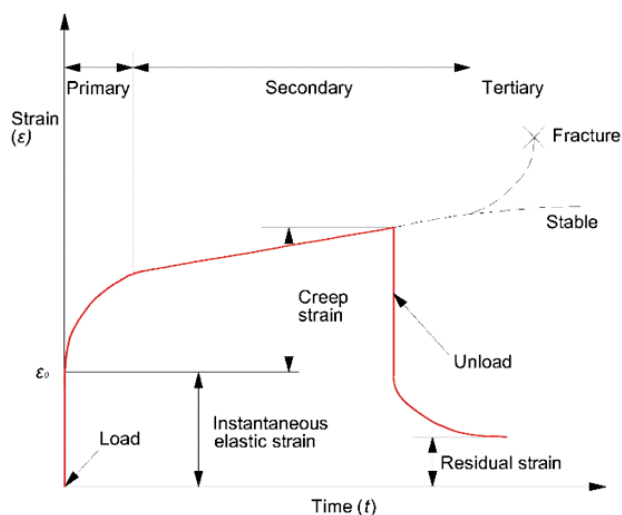


Figure 1. Time-strain curve and creep phases for specimen under constant load [33].

the secondary creep phase is characterised by a constant creep strain rate. The secondary creep phase is the longest of the entire creep processes and is usually observed as a linear strain rate. The final creep phase is tertiary creep, and it indicates a time-dependent deformation associated with crack growth and an increasing creep strain rate.

CREEP OF INTACT ROCK

The rheological parameters of different types of rocks have been comprehensively studied using numerous laboratory tests [3-6]. A few investigations have been performed on weak rocks, such as flysch rock masses [7-8] but the time-dependent behaviours of flysch rock cuts has never been thoroughly investigated.

Although the intact rock is generally part of a rock mass, it is very difficult to correlate the creep behaviour of intact rock and the time-dependent behaviour of a rock mass because of numerous associated variables such as the distribution, the frequency and creep characteristics of discontinuities, the scale effect, and the in situ stress distribution.

TIME-DEPENDENT BEHAVIOUR OF A ROCK MASS

Most of the studies conducted have been focused on the time-dependent behaviour of underground structures, whereas engineered slopes have been investigated in only a few studies. The behaviour of underground structures and slopes differs considerably because of many important factors, such as different stress fields, influence of weathering, pronounced inhomogeneity of layers and their parameters with depth, and increase in strength and deformability parameters with depth.

Panet [9] concluded that if very weak or heavily jointed or sheared rock is relatively homogeneous on a large scale, than it is reasonable to assume that the in situ rock mass

will follow trends similar to those obtained by laboratory tests. Several case studies have shown that there is no correlation between the creep parameters obtained from laboratory tests and the time-dependent behaviour of rock masses obtained from in situ measurements. To calibrate the equivalent rock mass creep parameters, Yu [10] used creep parameters obtained from laboratory tests (triaxial tests and a physical model of a tunnel) and concluded that even if there are significant differences between laboratory and in situ measured creep parameters, ratios between them and trends can be successfully determined.

The time-dependent behaviour of underground structures in rock masses has been detailed studied by many authors [9-18] while the time-dependent slope behaviour was less explored [19-23]. The time-dependent behaviour of reinforced cuts constructed in a weak rock mass, such as flysch, has never been investigated. In particular, the behaviour of the weathered profile as well as the variation in its strength, deformation, and creep properties has yet to be investigated.

2 WEATHERING OF A WEAK ROCK MASS

Weathering of a rock mass is a result of the destructive processes of atmospheric agents at or near the Earth's surface, whereas alteration is typically brought about by the action of hydrothermal processes. Both processes produce changes in the mineralogical composition of a rock, affecting colour, texture, composition, firmness, or form—features that result in a reduction of mechanical properties of a rock. Deterioration from weathering and alteration generally affects the walls of the discontinuities more than the interior of the rock [24]. During these processes, the fresh rock mass gradually transforms into residual soil – Fig. 2.

The description and classification of the state of weathering of a rock mass for engineering purposes has been

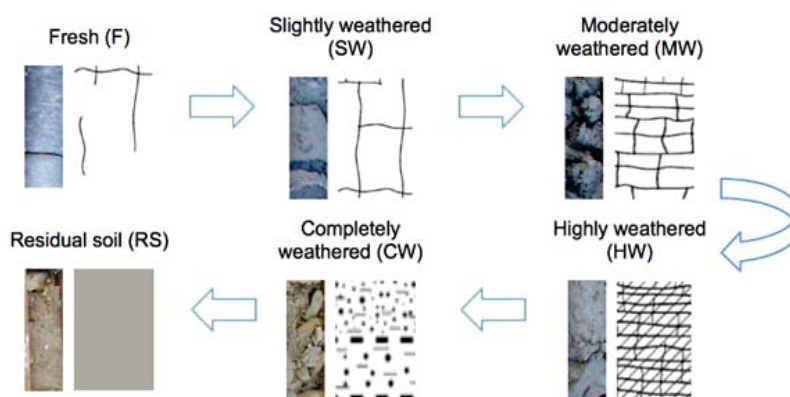


Figure 2. Process and grades of weathering in rock mass.

studied in detail by many authors [25-35]. Most of these classifications were established for a specific case, but the standard classification systems that have been recommended by several international committees are widely utilised and are most common in use: International Society for Rock Mechanics [36], British Standard Institution [37], the International Association of Engineering Geology [38].

Weak rock masses such as flysch have prominent weathering profiles below the surface that vary from residual soil (RS) and completely weathered (CW) rock mass near the surface, to highly weathered (HW) and moderately weathered (MW), to slightly weathered (SW) and fresh rock mass (F). A consequence of these different grades is a significant variation of the deformation and strength parameters with depth.

The deformation modulus for a rock mass weakened by weathering processes varies by several dozen times from low values for residual soils at the surface to very high values for a fresh rock mass in only a few meters of the weathering profile thickness. The strength reduction in slope layers due to the weathering of marl was investigated and numerically modelled by Eberhardt et al. [35] during the investigation of the Ruffi Landslide in Switzerland.

3 THE CASE STUDY OF DRAGA MOTORWAY

One of the most challenging sections of the Adriatic motorway along the Croatian Adriatic coast was constructed in the Draga Valley near the City of Rijeka during the period from 2004 to 2006. The Draga Motor-

way section is only 6.8 km long, but from geological, geotechnical, and construction points of view, it is a very complex transportation structure with 3 junctions, 2 tunnels, and several viaducts.

The major part of the motorway was constructed by cutting into the slopes made of a flysch rock mass. The stability of the cuts was established by reinforcing the rock mass with rockbolts and appropriate support systems such as multilayered shotcrete and reinforced concrete structures (Fig. 3).

GEOLOGICAL OVERVIEW

The geological fabric of the Draga Valley steep slopes is composed of limestone rock masses, and at the bottom of the valley, there are deposits of Paleogene flysch, which mainly consist of siltstone, with rare layers of sand, marl, and breccia. According to Arbanas et al. [39], the flysch rock mass is covered with slope formations, which tend to slide and denude the slope. The characteristic geological profile consists of clay cover originating from the disintegration of a flysch rock mass (RS) or brought gravitationally from hypsometrically higher parts of the slope, a layer of weathered flysch rock mass with variable characteristics that depend on the weathering stage (CW, HW, and MW), which significantly decreases with depth, and the fresh flysch zone as bedrock (SW and F).

WEATHERING PROFILE OF A FLYSCH ROCK MASS IN DRAGA VALLEY

The flysch rock mass in Draga Valley is mainly composed of a siltstone rock mass, which exhibits a visual transition from a completely weathered (CW) yellow coloured zone, through highly weathered (HW) and moderately

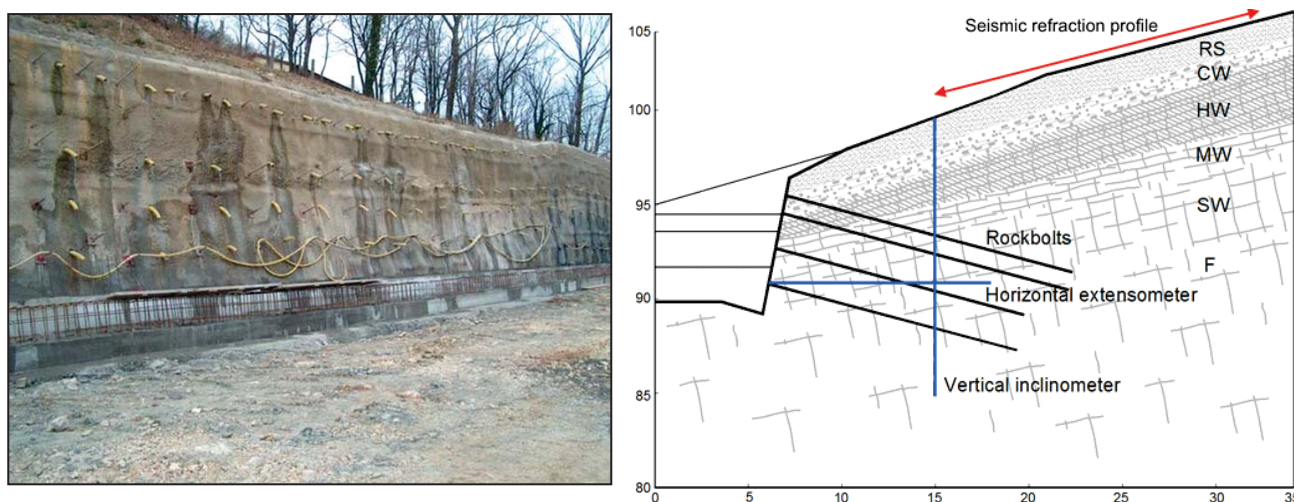


Figure 3. Reinforced cut in flysch rock mass at km 2+440.0: (left) during construction phase, and (right) cross section geometry.

weathered (MW), to the slightly weathered (SW) deposits and fresh rock mass (F) that are grey to blue (Fig. 2). In the zone of completely weathered siltstone, the rock mass is completely disintegrated, but the original structure of the rock mass is still intact. The layers of fresh siltstone have no visible weathering marks except for the colour change on the main discontinuity surfaces.

The weathering profile determination was based on geotechnical investigation, which consisted of drilling with core sampling, geophysical investigations, and laboratory tests. The depth of the weathering profile of the flysch rock mass with a complete transition from residual soil (RS) to fresh rock mass (F) was established as ranging from 5.0 to 8.0 m.

Determination of the geotechnical properties of the flysch rock mass during the geotechnical field investigations was difficult. During drilling, it was difficult to obtain undisturbed samples because of rock mass disintegration. Sudden degradation and disintegration of slightly weathered (SW) to fresh (F) siltstone occurred after removing geostatic loads and exposing the core to air and water. The consequence of these processes in the siltstone was that a very small number of undisturbed samples were taken for laboratory uniaxial strength tests.

There are other significant problems and unknowns when dealing with a heterogeneous flysch rock mass, which include vulnerability to weathering and sudden degradation and disintegration. These uncertainties include the following:

- The influence of weathering on reducing strength,
- Time dependence of weathering on reducing strength,
- Decrease in rock mass stiffness regarding the duration of the weathering process.

These unknowns are taken into account in geotechnical design by requiring higher safety factors and applying a conservative design approach based on limited experience.

GEOTECHNICAL INVESTIGATION RESULTS

Detailed geotechnical and geological studies of a flysch rock mass in Draga Valley were conducted and presented by Arbanas et al. [39-41].

The uniaxial strength of slightly weathered (SW) to fresh (F) siltstone obtained from uniaxial tests varied from 8 to 32 MPa. Obtaining undisturbed samples in completely (CW) to moderately weathered (MW) siltstone rock masses was not possible for the uniaxial test,

so point load tests (PLTs) were conducted immediately after drilling and sampling to avoid further weathering and strength reduction in the samples. A disadvantage of PLTs is the large dispersion of test results, which occurs especially in weak flysch rock masses. The use of this method is recommended when there is a lack of more reliable testing or a lack of appropriate representative samples and in combination with detailed descriptions of tested samples from the flysch rock mass. Test results of PLTs on fresh (F) siltstone samples showed that the representative uniaxial strength of these materials varies from 10 to 15 MPa, and in extreme cases, this value reached 20 MPa. The representative uniaxial strength of moderate (MW) to slightly weathered (SW) samples showed values <2 MPa. These values obtained from PLTs are uncertain and unacceptable for engineering analyses without adequate precautions.

The assessment of the strength parameters of the flysch rock mass was based on the Geological Strength Index (GSI) concept. Based on recommendations from Marinos and Hoek [42], a fresh (F) siltstone flysch rock mass from the Draga Valley slopes was placed in groups C to E, with GSI values from 10 to 30 [43], as shown in Fig. 4. The strength parameters are found to decrease as the weathering stage of the siltstone flysch rock mass increases, but the existing GSI estimate does not include the weathering grade as an influencing parameter that could affect the correction of the GSI value. This effect suggests the need for further evolution of the GSI concept in regard to different weathering categories of rock masses vulnerable to fast weathering processes.

Geophysical investigation involved seismic refraction and the downhole seismic survey method conducted during field investigations in the design phase. Additional geophysics investigations were performed at chainage 2+380.00 and 2+440.00 (Fig. 3) to obtain the thickness of the weathering profile of flysch and to investigate the distribution of shear wave's velocities through the weathering profile. Seismic refraction and a multichannel analysis of the surface wave method (MASW) were carried out at a length of 34.5 m with 24 channels and distances between geophones of 1.5 m. The results have shown that it is not possible to determine the disposition of the different grades of the weathering profile (from RS to F), but it is possible to determine the depth and the location of the fresh flysch rock mass – Fig. 5. Geophysics results were correlated with investigation drilling results and laboratory results, and it was observed that for longitudinal seismic wave velocities above 2,000.0 m/s, slightly weathered (SW) to fresh (F) flysch rock mass is present. Similar results were measured during field investigations at some other locations with similar geological profiles.

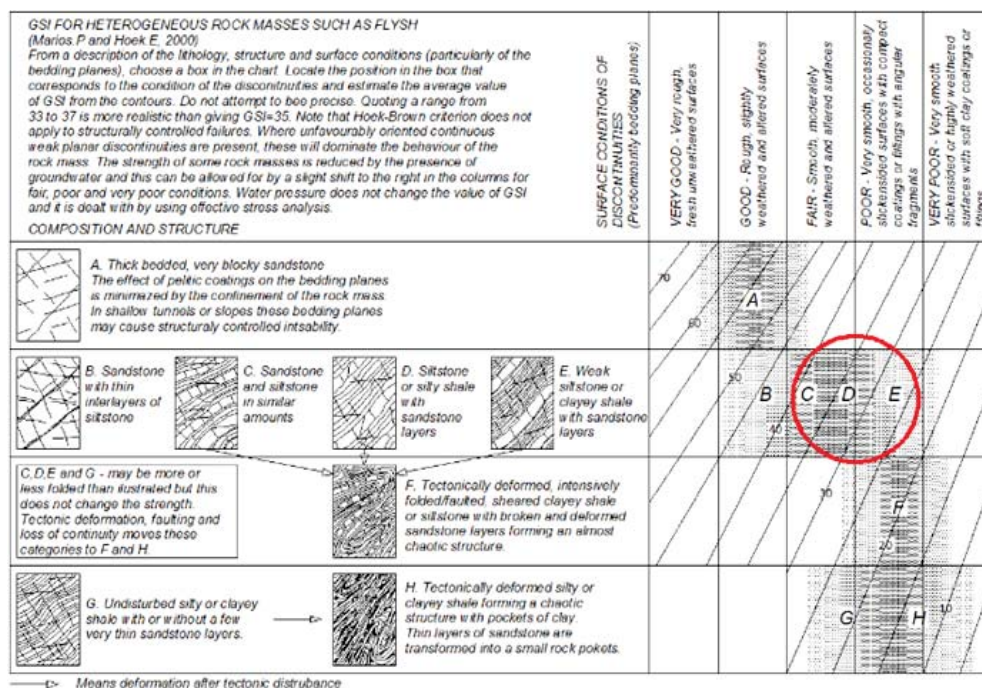


Figure 4. Properties of flysch rock mass in Draga Valley.

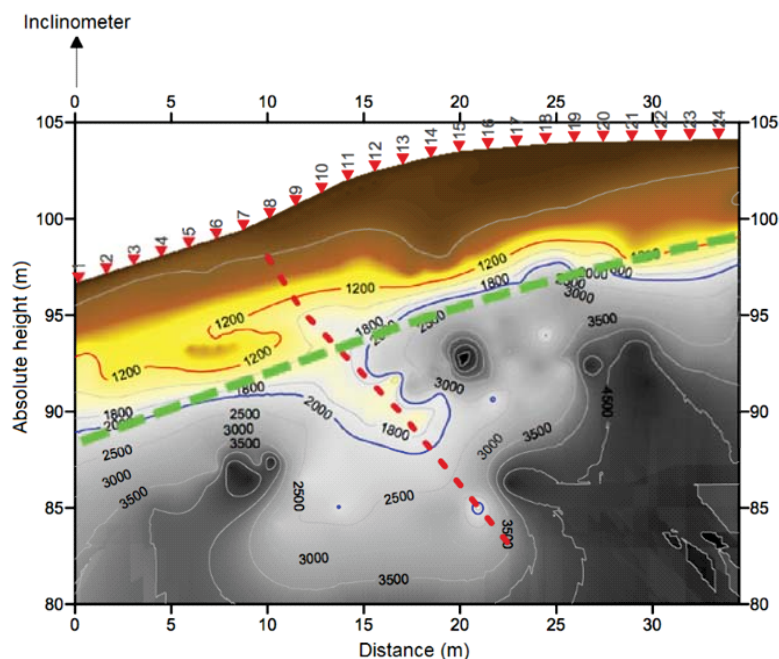


Figure 5. Longitudinal wave velocities obtained from seismic refraction measurement at chainage km 2+440.00 with marked border of SW to F flysch rock mass - green dashed line.

Geophysical investigations in correlation with other geotechnical investigations such as engineering geological core determination and classification and laboratory tests or in situ tests made it possible to determine the

borders of the slightly weathered (SW) and the fresh (F) flysch rock mass. This border also denotes the thickness of the weathering profile of the flysch rock mass, which is an important parameter for numerical analyses.

MONITORING DATA AND INTERPRETATION

The monitoring equipment were installed before construction included vertical inclinometers and horizontal extensometers installed in pairs, as shown in a cross section at chainage km 2+440.0, which was chosen as a representative cross section for the observation of the construction behaviour used in numerical analyses. Vertical inclinometer was installed in May 2004. and the reference measurement was carried out at 26th of May 2004., while the construction began at beginning of June 2004. The installed rockbolts were tested using pull-out tests, and the results of those tests made it possible to include the stiffness values of the installed anchors in numerical analyses.

The results of the horizontal displacement measurements at the vertical inclinometer at the chainage km 2+440.0 (Fig. 6) show that most of the displacement occurred in the upper part of the cut, i.e., in layers that

are characterised as residual soil (RS) to moderately weathered (MW) flysch rock mass. The maximum horizontal displacement occurred at the top of the inclinometer (6.0 mm), and the main part of these displacements occurred during the construction time period (3.9 mm) – marked in Fig. 6 as a dashed red line. The displacements that occurred during the exploitation period (2.1 mm) are significant and should not be neglected in the consideration of cut support stability analyses. Similar results were also obtained on other monitored profiles (0+560.0, 1+880.0, and 2+380.0), and it could be concluded that the delayed displacements reached up to 50% of the displacements that occurred during the construction time period – Table 2.

It is evident that most of the instantaneous displacements and time-dependent displacements occurred in the upper part of the cut and consisted of residual soil (RS) to moderately weathered (MW) flysch rock mass. A significant decrease of these displacements is observed as a function of the depth of the weathering profile of the flysch rock mass. Time-dependent displacements in the slightly weathered (SW) to fresh (F) flysch rock mass were not present and will not be considered and analysed in this research.

This transition between zones of different behaviour in the weathering profile of the flysch rock mass is evident and could be seen from monitoring results but also could be predicted from geotechnical investigation results.

3 MODELLING OF THE TIME – DEPENDENT BEHAVIOUR OF THE FLYSCH ROCK MASS

BACK ANALYSIS

According to Cividini et al. [44], there are two different ways to conduct back analyses: the inverse approach and the direct approach. For the inverse approach, the formulation is the reverse of that in ordinary stress analyses, even though the governing equations are identical. According to this approach, the number of measured values should be greater than the number of unknown parameters, but it is unclear whether the method could be applied in geotechnical problems in which the measured values contain scattering. The direct approach to back analysis is based on an iterative procedure of correcting the trial values of unknown parameters by minimising the error function. Gioda and Maier [45] noted that a significant advantage of the direct approach method is that it may be applied to non-linear back analysis without reliance on a complex

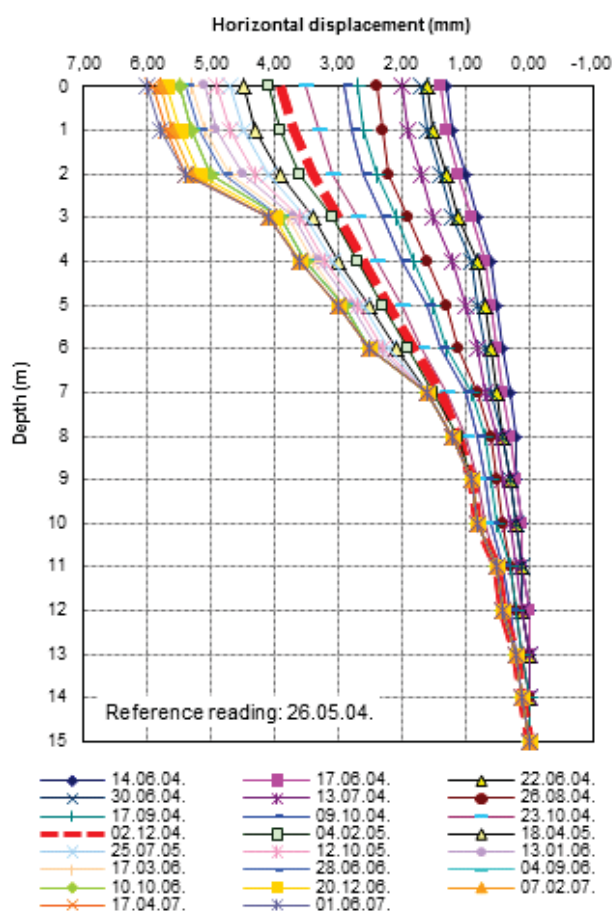


Figure 6. Measured horizontal displacements of vertical inclinometer installed at km 2+440.0 – end of construction phase is marked as dashed red line.

Table 2. Review of measuring results at monitoring profiles through motorway in Draga valley.

	Unit	0+560	1+880	2+380	2+440
Cut height	m	4.2	4.6	7.20	7.40
Inclinometer depth	m	15.0	15.0	15.0	15.0
Distance from the edge of the cut	m	15.5	9.5	10.5	8.5
End of construction date	-	09/17/04	05/03/03	12/02/04	12/02/04
Max. horizontal displacement (after construction phase)	mm	1.80	1.00	3.60	3.90
End of monitoring date	-	06/01/07	02/22/12	06/01/07	06/01/07
Max. horizontal displacement (after exploitation phase)	mm	6.40	1.90	5.40	6.00
Time period of monitoring in exploitation phase	days	1,053	2,672	901	901
Remark	-	Shallow sliding	-	-	-

mathematical background. Cividini et al. [454] stated that standard algorithms of mathematical programming might be adopted for numerical solutions. Iterative solutions require quite time-consuming computations.

VISCOPLASTIC BURGER MODEL

There are many rheological models used to describe the creep behaviour of rock or the time-dependent behaviour of the rock mass. These models can generally be divided into two main categories: the classic viscoplastic models and the viscoplastic-damaged models. The constitutive laws in the classic viscoplastic models relate the current strain rate to the current stress directly, where the relationship between the deviatoric strain rate and the deviatoric stress are schematically represented

by a series of spring, dashpot, and plastic slider elements connected in parallel and/or in series. The constitutive laws in the viscoplastic-damaged models are based on the principle of strain and energy equivalence and are derived from a standard thermodynamic dissipation potential. In this study, the Burger viscoplastic model was used within the software package FLAC V7.0 [46]. The selection of a more complex creep model could lead to more complex numerical analyses with a significant number of input parameters as unknowns but also could make a questionable contribution to the final results.

The classical elastoplastic Burger model, or the Burger-Mohr Coulomb model, can be described by the constitutive law that includes elastic volumetric and viscoplastic deviatoric behaviour [46]. The model is schematically presented in Fig. 7 and consists of the Kelvin unit, the Maxwell unit, and the Mohr Coulomb unit, which are serially connected.

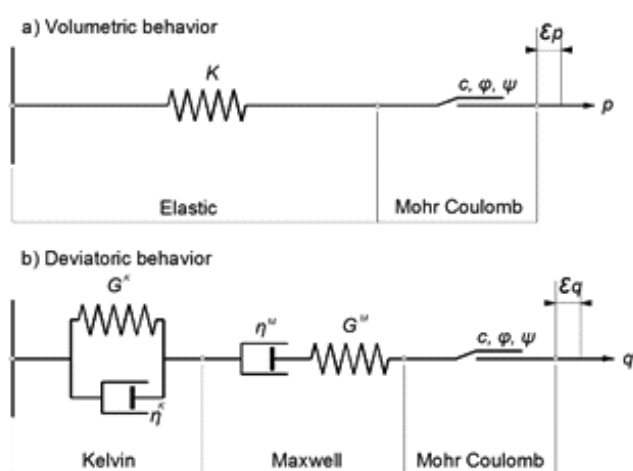


Figure 7. Sketch of Burger viscoplastic Mohr-Coulomb model: (a) volumetric behavior, and (b) deviatoric behavior [46].

The Kelvin unit is characterised by shear modulus G_K and viscosity η_K , the Maxwell unit by shear modulus G_M and viscosity η_M , and the Mohr-Coulomb unit by cohesion c , friction angle φ , and dilation angle ψ . The parameter G_K controls the total magnitude of the primary creep strain, or the so-called “delayed” elastic strain. A higher value of G_K denotes a lower amount of delayed strain, and the model tends to behave elastically in response to the applied stress. The viscosity parameter η_K controls the decaying rate of the primary creep strain of the material. A higher value of η_K denotes a longer time for the completion of the primary creep deformation phase. During the second creep phase, the parameter η_M controls the rate of increase of creep strain. A smaller value of this parameter denotes a more rapid increase of creep strain.

NUMERICAL ANALYSES

Numerical analyses and its results will be presented for the model established at the chainage 2+440; analyses conducted on other profiles (0+560.0, 1+880.0 and 2+380.0) showed similar results. Numerical analyses were performed in two phases: a construction phase (using elastoplastic Mohr-Coulomb model without taking into account time effects) and an exploitation phase (using Burger-Mohr-Coulomb model with taking into account time effects).

The numerical model used for the numerical analysis was divided into 7 different layers (geotechnical units) in reference to the geological weathering profile of the flysch rock mass. The disposition and thickness of these layers were defined based on geophysical measurements and longitudinal seismic wave velocities and divided into 7 groups: 0 – 400 – 800 – 1200 – 2000 – 3000 – 4000 m/s and higher, presented in Fig. 8. Those layers were described by different strength, deformability, and creep properties, which are summarised in Table 1. Similar determination of rock mass weathering grade in geological profile using seismic refraction method, MASW and electrical resistivity tomography method was presented in Olona et al. [47].

In the construction phase the slope was modelled using the linear elastoplastic Mohr-Coulomb model. Rockbolts in the model were defined as structural cables, with the stiffness obtained from in situ pull-out tests. Analyses were carried out in four stages, which represent excavation stages. After each stage, rockbolts and support construction installation were included in the model. The numerical model at the chainage 2+440 used for numerical analysis during the construction stage is presented in Fig. 8.

The back stress-strain analysis of the cut reinforced construction described above provided probable deformability parameter values: shear modulus, G , and bulk modulus, K , referring to the Mohr-Coulomb elastoplastic model. In the exploitation phase, the shear modulus, G , was used as the shear modulus of the Maxwell unit in the Burger model, G_M , whereas the shear modulus of the Kelvin unit, G_K , was taken as being ten times greater than G_M .

The exploitation phase analyses were carried out using the Burger-Mohr-Coulomb model for upper layers, denoted as RS, CW, HW, and MW, whereas the lower layers in the cut, denoted as SW and F, were modelled with the classic elastoplastic model and were not

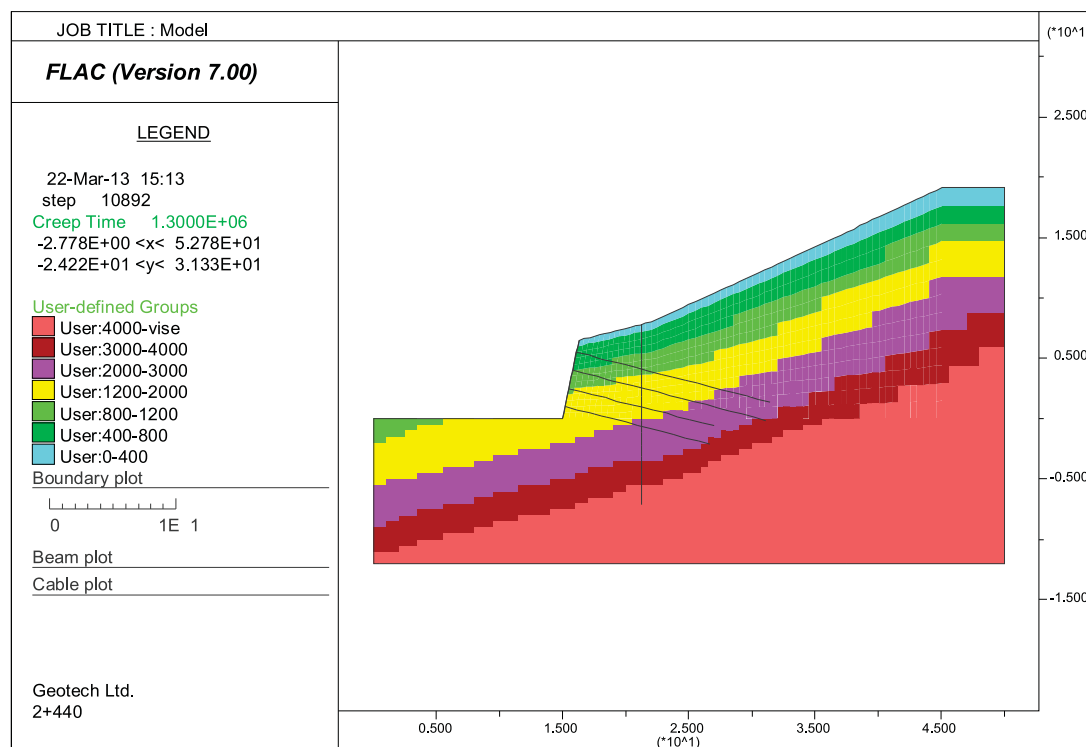


Figure 8. Numerical model at chainage km 2+440.0.

Table 1. Properties of different layers (geotechnical units) obtained from numerical back analysis of construction phase.

	Symbol	Unit	GU 1	GU 1	GU 3	GU 4	GU 5	GU 6	GU 7
Longitudinal wave velocity	v_p	m/s	0-400	400-800	800-1200	1200-2000	2000-3000	3000-4000	>4000
Weathering grade	-	-	RS-CW	CW-HW	HW-MW	MW-SW	SW-F	F	F
Model	-	-	CVISC	CVISC	CVISC	CVISC	MC	MC	MC
Cohesion	c	kPa	15	25	25	25	75	75	75
Friction angle	φ	o	25	32	32	32	32	32	32
Poisson coefficient	ν	-	0.25	0.25	0.25	0.25	0.25	0.25	0.25
Mass density	γ	kg/m ³	2,200	2,200	2,200	2,200	2,200	2,200	2,200
Shear modulus	G	kPa	6.0e2	1.8e3	6.0e3	1.8e4	1.8e4	3.0e4	4.8e4
Shear modulus of the Kelvin unit	G_K	kPa	3.0e3	9.0e3	3.0e4	9.0e4	-	-	-
Kelvin viscosity	η_K	kPamin	3.0e10	5.0e10	5.0e10	1.0e11	-	-	-
Maxwell viscosity	η_M	kPamin	3.0e12	5.0e12	5.0e12	1.0e13	-	-	-

processed as time dependent. The initial stress and strain states in the model were obtained from construction phase modelling.

The determination of the Burger model parameters for each geotechnical unit was the most challenging part of numerical analyses. Because of numerous uncertainties, a simplified method for parameter estimation in the first iteration was used: the shear modulus of the Maxwell unit, G_M , in the Burger model was referred to as a shear modulus, G , in the elastoplastic model obtained from a back analysis carried out from the construction phase. The shear modulus of the Kelvin unit, G_K , that controls primary creep is set to be five times higher than the shear modulus of the Maxwell unit, G_M (i.e., $G_K=5G_M$). The creep parameters of the viscosity of the Kelvin unit, η_K , and the Maxwell unit, η_M , were assumed to satisfy $\eta_M/\eta_K=100$. The values of the creep parameters of the viscosity of the Kelvin unit η_K were varied from 3e13 for GU 1, 5e13 for GU 2 and GU 3 and 10e13 kPa min for GU 4. The viscosity of the Maxwell unit η_M varied from 3e15 for GU 1, 5e15 for GU 2 and GU 3 and 10e15 kPa min for GU 4. Similar relationships were obtained from other studies [10, 15, 17, 18, 21, 23].

Using those relationships in the parameter selection, the number of parameters determined in the creep back analyses was considerably reduced.

Back analyses of the time-dependent behaviour of engineered slopes in the flysch rock mass were performed using a trial and error method to obtain the creep parameters of materials in the numerical model.

RESULTS OF NUMERICAL ANALYSES AND INTERPRETATION

Analyses were iterated until the values obtained from the inclinometer monitoring and the numerical model agreed. Using the technique described above, the deformation parameters were identified for 7 different layers of the cut weathering profile throughout the depth of the cut. Back analyses of the time-dependent behaviour of the reinforced cut enabled an estimation of creep parameters for 4 upper layers of the weathering profile. Those parameters ensured satisfactory adjustment of the numerical simulation results to field measurements for the different time periods presented in Fig. 9. The deformability and creep parameters obtained for the flysch rock mass in the analysed cuts were used for further simulations of time-dependent reinforced cut behaviour in the 50-year time period of the exploitation period – Fig. 10. Displacements gradually developed from the lower region to the top of the cut, with the tendency of displacement diminishing over the time.

Analyses have shown that the time-dependent behaviour of reinforced rock mass cuts resulted in stress-strain redistributions during the time period of exploitation and it has a significant influence on the rock cut reinforcing system. It is well known that the forces on rockbolts strictly depend on realised deformation in the cut, which consequently affect the cut stability expressed by the factor of safety.

Rockbolts in the rock cut support were activated during the construction phase as a consequence of initial rock bolt prestressing and the actual realised deformation

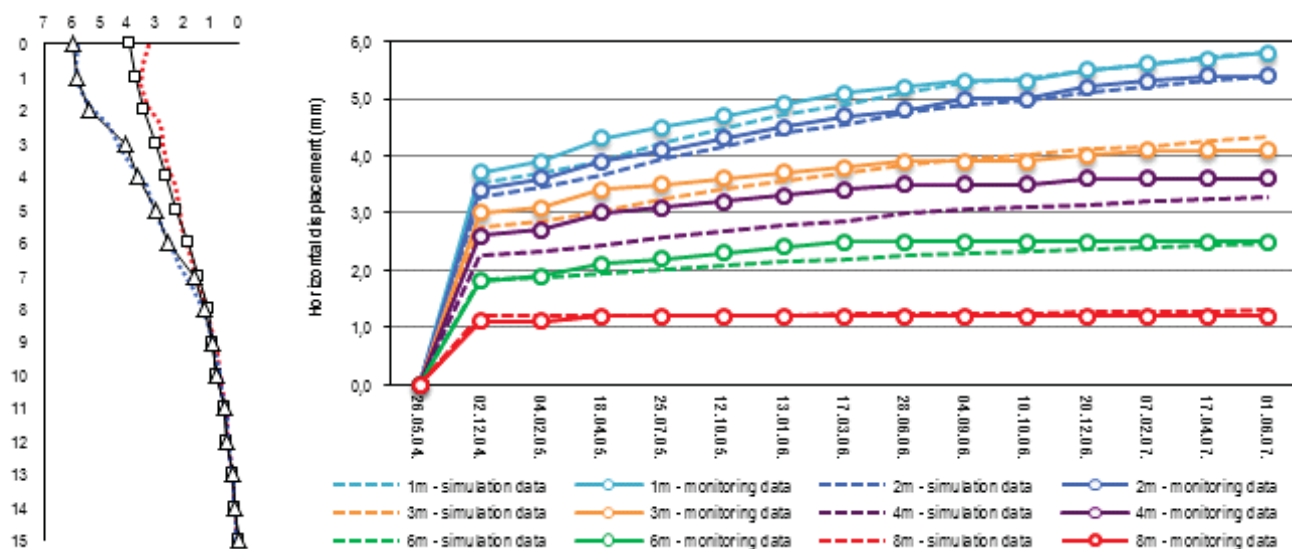


Figure 9. Results of numerical simulation and monitoring data at inclinometer at chainge km 2+440.0 (left) and displacements over time vs. depth of 1, 2, 3, 4, 6 and 8 m (right).

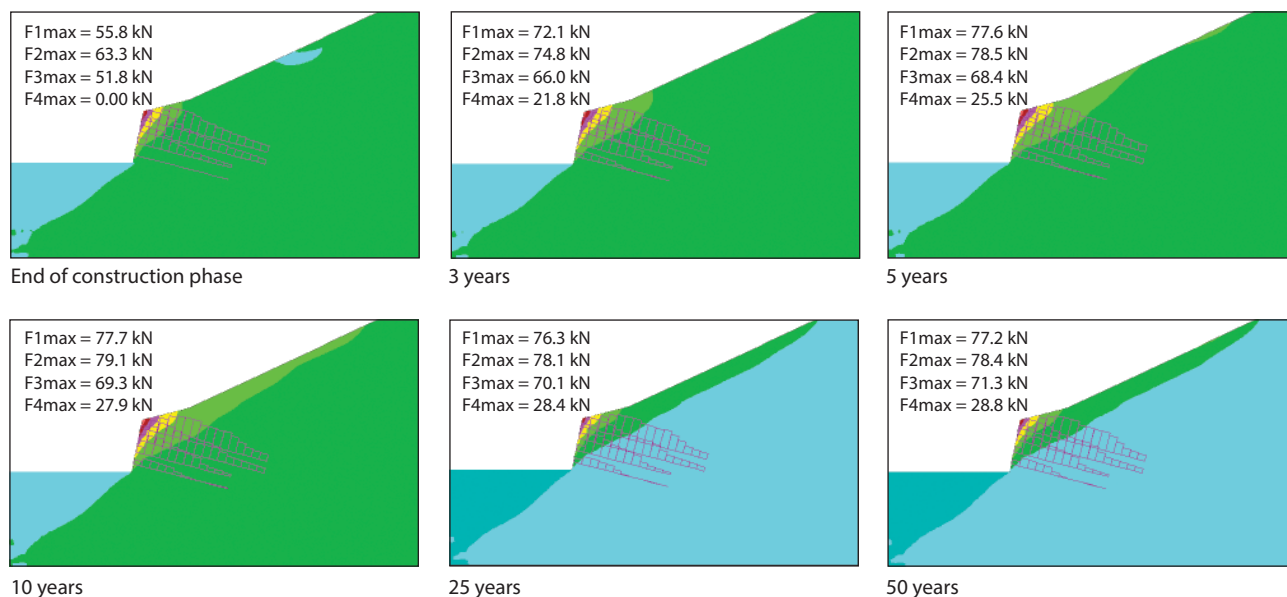


Figure 10. Propagation of horizontal displacements and axial forces distribution in rockbolts with maximal activated force in rockbolt during time period of 1, 3, 5, 10, 25 and 50 years.

in the cut due to excavation of consequent phases. In the case of no prestressing force in the fully grouted rockbolt, the lowest row of rockbolts, which was installed after the excavation was completed, was not activated, and the forces in the rockbolts were equal to

zero. The development of horizontal displacement over time consequently causes an increase in the forces on the rockbolts. The time-dependent behaviour of the reinforced cuts indicates that during the time period of exploitation, the stress and strain distribution affected

the activation of the bottom row of rockbolts and caused a significant redistribution of forces in all rockbolts and in the support construction – Fig. 10. It is noted that the axial forces in rockbolts increase during time. During time period of 5 years axial forces increase as follows: in the first (upper) row from 55.8 to 77.5 kN, in the second row from 63.3 to 78.4 kN, in the third row from 51.9 to 68.3 kN and in the fourth (bottom) row from 0.0 to 25.4 kN.

4 CONCLUSIONS

Flysch is categorised as a weak rock mass intensely subjected to weathering. Due to weathering processes, a flysch rock mass degrades from fresh rock to residual soil in only a few meters of the geological profile below the surface. This transition between different behaviours of the weathering profile of the flysch rock mass is evident and can be defined from geotechnical investigation results.

Displacements that occurred during the exploitation time period are significant and should not be neglected. It is evident that most parts of the instantaneous displacements and time-dependent displacements occurred in the upper part of the cut and consisted of residual soil (RS) to moderately weathered (MW) flysch rock mass layers. A significant decrease in these displacements is observed as a function of the depth of the flysch rock mass weathering profile. Parameters obtained from back analyses ensured satisfactory adjustment with numerical simulation results and field measurements for the different time periods.

In numerical analyses for geotechnical units from RS to MW, the shear modulus of the Kelvin unit, G_K that controls primary creep is set to be ten time higher than the shear modulus of the Maxwell unit, G_M . The creep parameters of the viscosity of the Kelvin unit, η_K , and the Maxwell unit, η_M , are taken as the ratio $\eta_M/\eta_K=100$. Using those relationships in parameter selection, the number of parameters determined in the creep back analyses was considerably reduced.

The development of displacement over time consequently causes an increase in the forces in the supporting systems such as rockbolts. The time-dependent behaviour of the reinforced cuts indicates that during the time period of exploitation, the stress and strain distribution affected the activation of the lowest row of rockbolts and caused a significant redistribution of forces in all other rockbolt rows and in the support construction.

REFERENCES

- [1] Hackley, A.V. and Ferraris, F.C. (2001). Guide to Rheological Nomenclature: Measurements in Ceramic Particulate Systems. NIST Special Publication 946, National Institute of Standards and Technology, Technology Administration, U. S. Department of Commerce
- [2] Andrade, E. (1910). The viscous flows in metals and allied phenomena. Proceedings of the Royal Society of London, Series A, Containing Papers of a Mathematical and Physical Character, Volume 84, Issue 567: 1-12
- [3] Maranini, E. and Brignoli, M. (1999). Creep behavior of a weak rock: experimental characterization. Int. J. of Rock Mechanics and Mining Sciences, Vol. 36, pp. 127-138.
- [4] Li, Y.S. and Xia, C.C. (2000). Time-dependent tests on intact rocks in uniaxial compression. Int. J. of Rock Mechanics and Mining Sciences, Vol. 37, pp. 467-475.
- [5] Fabre, G. and Pellet, F. (2006). Creep and time-dependent damage in argillaceous rocks. Int. J. of Rock Mechanics and Mining Sciences, Vol. 43, pp. 950-960.
- [6] Yang, S. and Jiang, Y. (2010). Triaxial mechanical creep behavior of sandstone. Mining Science and Technology, Vol. 20, pp. 339-349.
- [7] Tomanović, Z. (2006). Rheological model of soft rock creep based on the tests on marl. Mechanics of Time-dependent Materials, Vol. 10, pp. 135-154.
- [8] Fortsakis, P. and Kavvadas, M. (2009). Estimation of time dependent ground parameters in tunneling using back analyses of convergence data. Proc. Int. Conf. on Computational Methods in Tunneling, Ruhr University Bochum, Bochum
- [9] Panet, M. (1993). Understanding deformations in tunnels. Comprehensive Rock Engineering, Vol. 1, Pergamon Press.
- [10] Yu, C.W. (1998). Creep characteristics of soft rock and modelling of creep in tunnel. PhD Thesis, Department of Civil and Environmental Engineering University of Bradford, U.K
- [11] Gnirk, P.F. and Johnson, R.E. (1964). The deformational behavior of a circular mine shaft situated in a viscoelastic medium under hydrostatic stress. Proc. of 6th Symposium of Rock Mechanics, University of Missouri Roll.
- [12] Sakurai, S. (1978). Approximate time-dependent analysis of tunnel supports structure considering progress of tunnel face. Int. J. for Numerical Analytical Methods in Geomechanics, Vol. 2, pp. 159-175.

- [13] Gioda, G. (1981). A finite element solution of non-linear creep problems in rock. *Int. J. of Rock Mechanics and Mining Sciences & Geomechanics Abstracts*, Vol. 8, pp. 35–46.
- [14] Ladanyi, B. and Gill, D. (1984). Tunnel lining design in creeping rocks. *Proc. of Symposium on Design and Performance of Underground Excavations*, ISRM, Cambridge.
- [15] Goodman, R. E. (1989). *Introduction to Rock Mechanics*, Wiley, New York.
- [16] Likar, J. (2004). Back analyses of time-dependent displacement at the Trojane tunnel construction. *Acta Geotechnica Slovenica*, Vol. 1, pp. 21–36.
- [17] Likar, J., Vesel, G., Dervarič, E. and Jeromel, G. (2006). Time-Dependent Processes in Rocks. *RMZ – Materials and Geoenvironment*, Vol. 53, No. 3, pp. 285–301.
- [18] Guan, Z., Jiang, Y., Tanabashi, Y. and Huang, H. (2008). A new rheological model and its application in mountain tunneling. *Tunnelling and Underground Space Technology*, Vol. 23, pp. 292–299.
- [19] Martin, C.D. (1993). Time dependent behavior of rock slopes. PhD Thesis, University of London.
- [20] Feng, J., Chuhan, Z., Gang, W. and Guanglun, W. (2003). Creep Modeling in Excavation Analysis of a High Rock Slope. *J. of Geotechnical and Geoenvironmental Engineering*, Vol. 129, pp. 849–857.
- [21] Apuani, T., Masetti, M. and Rossi, M. (2007). Stress–strain–time numerical modelling of a deep-seated gravitational slope deformation: Preliminary results. *Quaternary International*, Vol. 171–172, pp. 80–89.
- [22] Kodama, J., Nishiyama, E. and Kaneko, K. (2009). Measurement and interpretation of long-term deformation of a rock slope at the Ikura limestone quarry, Japan. *Int. J. Of Rock Mechanics and Mining Sciences & Geomechanics Abstracts*, Vol. 46, pp. 148–158.
- [23] Bozzano, F., Martino, S., Montagna, A. and Prestinzi, A. (2011). Back analysis of a rock landslide to infer rheological parameters. *Engineering Geology*, Vol. 131–132, pp. 45–56.
- [24] Piteau, D.R. (1970). Geological factors significant to the stability of slopes cut in rock. *Proc. Symp. on Planning Open Pit Mines*, Johannesburg, South Africa.
- [25] Vargas, M. (1953). Some engineering properties of residual clay soils occurring in southern Brazil. *Proc. of the 3rd International Conference on Soil Mechanics and Foundation Engineering*, Zurich, Vol. 1, pp. 259–268.
- [26] Ruxton, B.P. and Berry, L. (1957). Weathering of granite and associated erosional features in Hong Kong. *Bulletin of Geological Society of America*, Vol. 68, pp. 1263–1292.
- [27] Ward, W.H., Burland, V.B. and Gallois, R.W. (1968). Geotechnical assessment of a site at Mundford, Norfolk for a large proton accelerator. *Géotechnique*, Vol. 18, pp. 399–431.
- [28] Chandler, R.J. (1969). The effect of weathering on the shear strength properties of Keuper marl. *Géotechnique*, Vol. 19, pp. 321–334.
- [29] Saunders, M.K. and Fookes, P.G. (1970). A review of the relationship of rock weathering and climate and its significance to foundation engineering. *Engineering Geology*, Vol. 4, pp. 289–325.
- [30] Fookes, P.G. and Horswill, P. (1970). Discussion on engineering grade zones. *Proc. of the In Situ Investigations in Soils and Rocks*, London, pp. 53–57.
- [31] Knill, J.L., Cratchley, C.R., Early, K.R., Gallois, R.W., Humphreys, J.D., Newbery, J., Price D.G. and Thurrell, R.G. (1970). The logging of rock cores for engineering purposes. *Geological Society Engineering Group Working Party Report, Quarterly Journal Engineering Geology*, Vol. 3, pp. 1–24.
- [32] Geological Society of London (1972). The preparation of maps and plans in terms of engineering geology. *Geological Society Engineering Group Working Party Report, Quarterly Journal Engineering Geology*, Vol. 5, pp. 293–382.
- [33] Lama, R.D. and Vutukuri, V.S. (1978). *Handbook on mechanical properties of rocks*. Trans Tech Publications, Clausthal, Germany.
- [34] Sancio, R.T. and Brown, I. (1980). A classification of weathered foliated rocks for use in slope stability problems. *Proc. of the 3rd Australia – New Zealand Conference on Geomechanics*, Wellington, Vol. 2, pp. 81–86.
- [35] Eberhardt, E., Thuro, K. and Luginbuehl, M. (2005). Slope instability mechanisms in dipping interbedded conglomerates and weathered marls – the 1999 Ruffi landslide, Switzerland. *Engineering geology*, Vol. 77, pp. 35–56.
- [36] ISRM (1978). Suggested methods for the quantitative description of discontinuities in rock masses. *Int. J. of Rock Mechanics Mining Sciences and Geomechanics Abstracts*, Vol. 15, pp. 319–368.
- [37] BSI (1981). *Code of Practice for site investigations*, BS 5930. British Standards Institution, London, p. 147.
- [38] IAEG (1981). Rock and soil description and classification for engineering geological mapping. *Bulletin of International Association of Engineering Geology*, Vol. 24, pp. 253–274.
- [39] Arbanas, Ž., Benac, Č., Andrić, M. and Jardas, B. (1994). Geotechnical Properties of Flysch on the Adriatic Motorway from Orehovica to St. Kuzam.

- Proc. of the Symposium of Geotechnical Engineering in Transportation Projects, Croatian Geotechnical Society, Vol. 1, pp. 181-190.
- [40] Arbanas, Ž., Grošić, M. and Jurić-Kaćunić, D. (2007). Experiences on flysch rock mass reinforcing in engineered slopes, The Second Half Century of Rock Mechanics. Proc. of the 11th Congress International Society for Rock Mechanics, Lisbon, Portugal, pp. 597-600.
- [41] Arbanas Ž, Grošić M, Dugonjić S (2008). Behaviour of the reinforced cuts in flysch rock mass, Proc. of 1st Int. Conf. On Transportation Geotechnics, Nottingham, UK, pp. 283-291.
- [42] Marinos, P. and Hoek, E. (2001). Estimating the Geotechnical Properties of Heterogeneous Rock Masses such as Flysch. Bulletin of Engineering Geology and the Environment, Vol. 60, pp. 85-92.
- [43] Brunčić, A., Arbanas, Ž. and Kovačević, M.-S. (2009). Design of engineered slopes in flysch rock mass, Proc. Int. Conf. on Soil Mechanics and Geotechnical Engineering.
- [44] Cividini, A., Jurina, L. and Gioda, G. (1981). Some Aspects of Characterization Problems in Geomechanics. Int. J. Of Rock Mechanics and Mining Sciences & Geomechanics Abstracts, Vol. 18, pp. 487-503.
- [45] Gioda, G. and Maier, G. (1980). Direct Search Solution of an Inverse Problem in Elastoplasticity: Identification of Cohesion, Friction Angle and In-situ Stress by Pressure Tunnel Tests. Int. J. For Numerical Methods in Engineering, Vol. 15, pp. 1823-1848.
- [46] Itasca Consulting Group Inc. (2011). FLAC, Fast Lagrange Analysis of Continua, Version 7.0, User Manual, Minneapolis.
- [47] Olona, J., Pulgar, A. J., Fernández-Viejo, G., López-Fernández, C. and González-Cortina, J. M. (2009) Weathering variations in a granitic massif and related geotechnical properties through seismic and electrical resistivity methods. Near Surface Geophysics, Vol. 8, pp. 585-599